


ORIGINAL ARTICLE

Recombinant Newcastle disease virus expressing human IFN- λ 1 (rL-hIFN- λ 1)-induced apoptosis of A549 cells is connected to endoplasmic reticulum stress pathways

Yulan Yan^{1,2}, Sha Liu^{1,2}, Mi Li², Yinghai Zhao², Xiaomei Shao², Min Hang² & Xuefeng Bu³ 

1 Department of Respiratory Medicine, Affiliated People's Hospital of Jiangsu University, Zhenjiang, China

2 Clinical Medicine College, Jiangsu University, Zhenjiang, China

3 Department of General Surgery, Affiliated People's Hospital of Jiangsu University, Zhenjiang, China

KeywordsApoptosis; ER stress; IFN- λ 1; lung cancer; recombinant Newcastle disease virus (NDV).**Correspondence**

Xuefeng Bu, Department of General Surgery, Affiliated People's Hospital of Jiangsu University, DianLi Road No.8, Zhenjiang, Jiangsu 212002, China.

Tel: +86 139 5281 9838

Fax: +86 139 8523 4387

Email: xuefengbu05@163.com

Received: 28 May 2018;

Accepted: 2 August 2018.

doi: 10.1111/1759-7714.12857

Thoracic Cancer 9 (2018) 1437–1452

Abstract

Background: IFN- λ s are a kind of cytokine with anti-tumor, immunomodulatory, and anti-proliferative activity. Recent studies have shown that the recombinant Newcastle disease virus expresses human IFN- λ 1 (rL-hIFN- λ 1), which plays a role in gastric cancer cell apoptosis. Endoplasmic reticulum stress (ERS) induces autophagy and apoptosis in tumor cells. In this study, we explored the relationship between ERS and rL-hIFN- λ 1-induced apoptosis of lung adenocarcinoma A549 cells and its underlying mechanism.

Methods: First, we investigated the effect of rL-hIFN- λ 1 on cellular proliferation, migration, and proteins associated with ERS, autophagy, and apoptosis of A549. Second, after administration of the ERS inhibitor, the associated proteins induced by rL-hIFN- λ 1 were detected. Finally, a subcutaneous mouse model was used to examine the effect of rL-hIFN- λ 1 on tumor growth and the ERS and apoptosis associated proteins in tumor tissues.

Results: The results showed that the proliferation and migration of A549 cells, and tumor tissue growth were significantly inhibited and the ERS, autophagy, and apoptosis associated proteins were upregulated in the experimental group. Additionally, both 4-PBA and knockdown of PERK or CHOP reduced the levels of rL-hIFN- λ 1-induced autophagy and apoptosis-associated proteins. BCL-2 knockdown caused autophagy and apoptosis associated protein upregulation.

Conclusions: In summary, rL-hIFN- λ 1 inhibited cell proliferation and activated ERS, autophagy, and apoptosis in A549 cells and tissues, and when ERS pathways were blocked, the inhibiting effect was even more pronounced. Therefore, the recombinant Newcastle disease virus rL-hIFN- λ 1-induced apoptosis of A549 cells is connected to ER stress and could be a promising therapeutic agent for lung adenocarcinoma.

Introduction

Lung cancer, including small cell lung carcinoma and non-small cell lung carcinoma, is the most common cause of cancer death worldwide.¹ Non-small cell lung carcinoma is the most common type, accounting for 40% of lung cancer cases. In recent decades, the incidence of lung adenocarcinoma has been increasing in many developed Western nations.^{2–5} In spite of advanced treatments, such as radiotherapy, chemotherapy, and surgery, the five-year survival

rate for advanced stage lung adenocarcinoma is only 5–20%. Therefore, novel approaches are required to improve clinical outcomes.

Oncolytic Newcastle disease viruses (NDV) and avian paramyxovirus replicate selectively and destroy tumor cells.⁶ The effective antiviral characteristics of normal cells make NDV a safe and effective anticancer drug.⁷

Type III IFN- λ s, which are similar to type I IFN λ s, play an important role in cancer and viral disease treatment.

However, type I IFN λ s are hampered in clinical practice by a wide range of adverse effects.⁸ IL-29, namely IFN- λ 1, belongs to the family of type III IFN λ s, which include IFN- λ 1, IFN- λ 2, and IFN- λ 3, also known as IL-29, IL-28A and IL-28B, respectively.⁹ Recent data have indicated that IFN- λ 1 might serve as a potential therapeutic agent for certain cancer types.¹⁰

Our team previously reported that recombinant adenovirus Ad-mIFN- λ 2 inhibited growth and triggered the apoptosis of A549 cells. Recently, our research indicated that recombinant NDV expressing the rabies virus glycoprotein (rL-RVG) could induce endoplasmic reticulum stress (ERS), which contributes to apoptosis in satellite glial and human cell line cells.¹¹ Furthermore, we successfully constructed recombinant NDV-expressing human IFN- λ 1 (rL-IFN- λ 1) and found that it could induce apoptosis in gastric adenocarcinoma cells.¹² In this study, we investigated the relationship between A549 cell apoptosis induced by recombinant NDV rL-hIFN- λ 1 and ERS, and as its associated pathways.

Considering that rL-hIFN- λ 1 could induce ERS in lung cancer, we analyzed the expression of representative ERS, autophagy, and apoptosis associated proteins in rL-hIFN- λ 1-infected A549 cells with or without pretreatment of small interfering (si)PERK, siCHOP, or siBCL-2. Furthermore, tumor-bearing mice with lung adenocarcinoma A549 cells were also infected with rL-hIFN- λ 1, and its effect on the apoptosis of A549 cells and the related mechanism was explored. Our results indicated that rL-hIFN- λ 1 plays a key role in mediating the ERS response and apoptosis in A549 cells, as well as tumor tissues. Moreover, in this study, the underlying relationships among ERS, autophagy, and apoptosis were also clarified.

Methods

Reagents

Construction of the recombinant NDV strain (rL-hIFN- λ 1) was supported by the Harbin Veterinary Research Institute (Harbin, Heilongjiang, China),¹² which also kindly provided the wild-type NDV LaSota strain. The human lung adenocarcinoma A549 cell line, the human lung squamous carcinoma SK-MES-1 cell line, and the mouse adenocarcinoma Lewis cell line were obtained from Shanghai Cell Bank (Shanghai, China). Methyl-thiazolyl-tetrazolium (3-[4,5-dimethylthiazol-2-yl]-2,5-diphenyltetrazolium bromide, MTT), 4-phenylbutyric acid (4-PBA), and the JNK inhibitor SP600125 were purchased from Sigma-Aldrich (St. Louis, MO, USA). Antibodies against GRP78, CHOP, p-eIF2 α , hIFN- λ 1, and β -actin antibodies were purchased from Santa Cruz Biotechnology (Santa Cruz, CA, USA). Antibodies against p-PERK, beclin 1, caspase3, caspase8,

and caspase9 were obtained from Boster Biological Technology (Wuhan, Hubei, China). Antihuman IL-28R monoclonal antibody (mAb) was obtained from R&D Systems (Minneapolis, MN, USA). SiRNAs against human CHOP, PERK, and BCL-2 were synthesized by GenePharma (Shanghai, China). Male BALB/c nude mice, aged 3–4 weeks of age and free of murine-specific pathogens were obtained from the Laboratory Animal Center, Yangzhou University (Yangzhou, China). The nude mice were treated twice weekly by subcutaneous instillation with 300 μ l of rL-hIFN- λ 1, NDV, and phosphate buffered saline (PBS), respectively. Biologend (San Diego, CA, USA) provided fluorescein isothiocyanate (FITC)-anti-mouse cluster of differentiation CD49b and CD3. An enzyme-linked immunosorbent assay

(ELISA) kit for detecting IFN- λ 1 was purchased from e-Bioscience (San Diego, CA, USA).

Enzyme-linked immunosorbent assay (ELISA) analysis

A549 cells were cultured in Dulbecco's modified Eagle medium containing 10% fetal bovine serum at 37°C with 95% humidified air and 5% CO₂, and incubated with rL-hIFN- λ 1, NDV, or PBS for 24 hours. The supernatants of A549 cells were collected, and the hIFN- λ 1 levels in supernatants were measured using an ELISA kit.

Methyl-thiazolyl-tetrazolium (MTT) assay

Cell viability was detected using MTT assay. First, cells were seeded into a 96-well flat bottom microplate at a density of 1×10^5 cells in 100 μ L per well. Lung adenocarcinoma A549 cells were infected with rL-hIFN- λ 1 or NDV at different multiplicities of infection (1.25, 2.5, 5.0, and 10.0, respectively). After 24 hours, the cells were evaluated under a microscope and cell proliferation was assessed by measuring the conversion of the tetrazolium salt to formazan according to the manufacturer's instructions (Sigma). The cells were then incubated for four hours at 37°C, 150 μ L of dimethyl sulfoxide was added to each well, and the absorbance of the solution was analyzed at an absorbance of 450 nm. The following equation was used to calculate cell viability: $(1 - A_{450} \text{ sample absorbance} / A_{450} \text{ control absorbance}) \times 100\%$.

Clonogenic survival assay

A549 cells were plated in six-well plates (1500 cells per well) and cultured overnight before being transfected with or without siRNA. Four hours later, the cells were treated with rL-hIFN- λ 1, NDV, or PBS for 24 hours. Several days later the medium was replaced with virus-free medium and

the cells were fixed and stained with crystal violet (0.2%) to visualize cell colonies. Each experiment was repeated three times.

Scratch migration

When A549 cells reached 80–90% confluence, 10 μ L sterile tips were used to draw a straight line in each well. The cells were then infected with rL-hIFN- λ 1, NDV, or PBS. Each experiment was repeated three times. Twenty-four hours later, the substance in each well was replaced with serum-free Dulbecco's modified Eagle medium and was monitored regularly.

Transwell

To achieve a steady growth state, cells were maintained for 24 hours in serum-free medium prior to treatment with rL-hIFN- λ 1 or NDV for another 24 hours. Cells (1.5×10^5 cells/mL) were then plated onto transwell filters in a 24-well plate, according to the manufacturer's instructions. Finally, cells were fixed with 4% paraformaldehyde, stained with crystal violet (0.2%), and monitored under a microscope.

Transmission electron microscopy

After infection for 24 hours with rL-hIFN- λ 1, NDV, or PBS, A549 cells were fixed and embedded in 4% paraformaldehyde and 2.5% glutaraldehyde. Finally, thin sections were cut and examined using an H-600 transmission electron microscope.

Western blot analysis

After treatment with or without 4-PBA, siPERK, siCHOP, siBCL-2, and JNK inhibitor, cells were extracted in lysis buffer (containing 2 \times loading buffer, β -mercaptoethanol) with complete protease inhibitor (Boster Biological Technology). Lysates were centrifuged at 12000 rpm for five minutes. Supernatants were collected, subjected to electrophoresis on 12% polyacrylamide gel (for light chain LC3 and caspase3 antibodies) or 10% polyacrylamide gel (for NDV, hIFN- λ 1, IL-28R, GRP78/Bip, CHOP, p-eIF2 α , beclin1, caspase8, caspase9, p-PERK, BCL-2, and Bax antibodies) and then transferred to Immobilon-P membranes (Millipore, Temecula, CA, USA). The blot was blocked in 5% non-fat dry milk for 60 minutes and incubated overnight at 4°C with appropriate primary antibodies. The blot was then incubated with appropriate secondary antibodies at room temperature for 1.5 hours. Finally, protein bands were visualized with electrochemiluminescence.

Small interfering RNA transfection

When the cells reached 50% confluence, GenePharma siRNA transfection reagent was used. The lung cancer A549 cells pretreated with siPERK, siCHOP, or siBCL-2 were infected for 24 hours with rL-hIFN- λ 1, NDV, or PBS, respectively. Thereafter, the cells were analyzed by immunoblot to validate the knockdown efficiency.

Immunofluorescent staining

A549 cells were seeded in 24-well plates and incubated overnight. After treatment with rL-hIFN- λ 1 or NDV for 24 hours, the cells reached 50% confluence. The cells were fixed in 4% paraformaldehyde, and were then permeabilized with 0.1% TritonX-100 for 20 minutes. After cells were washed with PBS for 10 minutes, they were blocked in 1% normal goat serum for one hour. They were then incubated in a 4°C wet box overnight with anti-GRP78 (Santa Cruz Biotechnology), anti-CHOP (Santa Cruz Biotechnology), NDV F protein (Harbin Veterinary Research Institute), and hIFN- λ 1 (Santa Cruz Biotechnology) antibodies, respectively. After being washed with PBS three times, cells were stained with appropriate secondary antibodies. The nuclei were stained with Hoechst 33 342 for 30 minutes (Sigma) and the cells were then observed under a microscope.

Reverse transcriptase PCR splicing assay

According to the manufacturer's instructions, total RNA was extracted with TRIzol reagent and complementary DNA was generated using oligo (dT) primers and MultiScribe reverse transcriptase. Amplification of hIFN- λ 1 cDNA was performed with 5'-TATCCAGCCTCAGCCCA-CAGCA-3' (sense) and 5'-ACAGGTTCCCATCGG CCACATA-3' (anti-sense) primers.

Construction of a subcutaneous tumor-bearing mouse model

To construct a subcutaneous tumor-bearing mouse model, 2.0×10^6 lung adenocarcinoma A549 cells in 200 μ L of PBS were injected into the left oter of four-week-old male BALB/c mice. A few days later, the subcutaneous tumor was observable.

Curve of tumor volume and weight of tumor-bearing mice

Two weeks later, tumors under the left oter of each mouse, measuring 5–15 mm in diameter, were observed. The tumor-bearing mice were randomly divided into rL-

hIFN- λ 1, NDV, and control groups and received 300 μ L of rL-hIFN- λ 1, NDV, or PBS, respectively, twice weekly (Thursday and Saturday) for four weeks. The tumor volumes were measured. A growth curve of the tumor volume was calculated using the following formula: volume = $a^2 \times b \times 0.52$, where a and b refer to the short and long diameters of the tumors, respectively. Tumor inhibition rate = (average tumor volume in control group - average tumor volume in treatment group) / mean tumor volume in control group $\times 100\%$.

Flow cytometry

Apoptosis was analyzed using flow cytometry. After being digested, centrifuged, collected, washed, and resuspended, A549 cells were fixed with 70% ethanol precooled at 4°C for 30 minutes. The cells were then centrifuged and washed with PBS, and the fixed cells were treated with a ribonuclease solution for 30 minutes. After staining with Annexin V-FITC and propidium iodide, flow cytometry was used to examine apoptosis. Finally, all data were analyzed using FlowJo software (Tree Star Inc., Ashland, OR, USA). Flow cytometry assay was also used to detect natural killer (NK) cells. Splenocyte suspensions were obtained from the spleens of the sacrificed mice and the splenocytes (100 μ L aliquots) were labeled with 2 μ L of CD49b-FITC and 1.25 μ L of hamster CD3e-phycoerythrin. The number of CD3-/CD49+ NK cells was detected using flow cytometry. Each experiment was performed three times.

Immunohistochemistry

Experiments were performed on tumor tissues from tumor-bearing mice with the appropriate primary IFN- λ 1 and NDV antibodies (1:200) and secondary (horseradish peroxidase-conjugated anti-rabbit or anti-chicken) antibodies, as previously described.⁵

Sample collection and pathological examination

The harvested tumor specimens were fixed in 4% paraformaldehyde and embedded in paraffin. Hematoxylin and eosin staining was performed to identify morphology changes.

Statistical analyses

All analyses were performed using SPSS version 17.0 (SPSS Inc., Chicago, IL, USA). One-way analysis of variance and Student's *t* tests were used to evaluate the significance of statistical differences. *P* values < 0.05 or < 0.01 were considered significant.

Results

hIFN- λ 1, Newcastle disease virus (NDV), and IL-28R protein expression levels

We first examined the expression of the receptor subunits for type III IFN in A549, SK-MES-1, and Lewis cell lines. The receptor complex of type III IFN signals consists of IL-10Rb and IL-28R. IFN- λ 1 may have a relatively high affinity to IL-28R.^{13,14} In this study, we used Western blot analysis to detect IL-28R expression in A549, SK-MES-1, and Lewis lines (data shown in Fig 1a). A549 cell lines displayed higher levels of surface IL-28R expression than the SK-MES-1 and Lewis lines (Fig 1a). As a result, the A549 cell line was selected for use in further experiments.

hIFN- λ 1 expression was then detected by using an ELISA kit, according to the manufacturer's instructions. Supernatants of A549 cells in the NDV and rL-hIFN- λ 1 groups were diluted 800-fold, 400-fold, 200-fold, and 100-fold. ELISA analysis of the PBS group revealed almost no hIFN- λ 1 expression in the supernatant compared to the rL-hIFN- λ 1 and NDV groups. In addition, hIFN- λ 1 was significantly higher in the rL-hIFN- λ 1 than in the NDV group (Fig 1b).

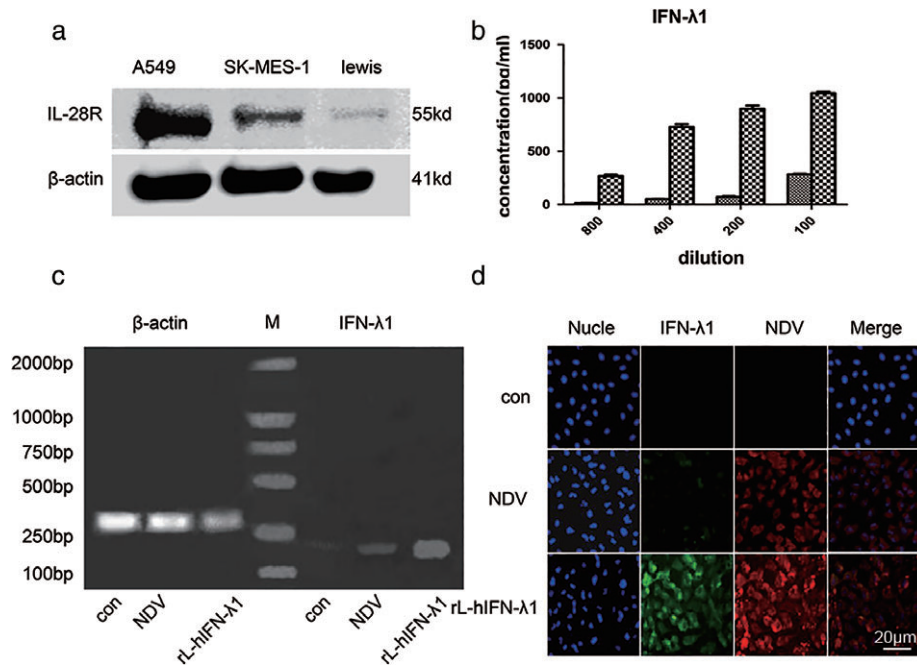
To explore the effects of hIFN- λ 1 transfection, reverse transcriptase (RT)-PCR was performed to detect hIFN- λ 1 messenger RNA (mRNA) expression in A549 cells. hIFN- λ 1 mRNA was highly expressed in the rL-hIFN- λ 1 group, but was relatively lower in the PBS and NDV groups (Fig 1c). These findings strongly indicate that hIFN- λ 1 is stably expressed in the rL-hIFN- λ 1 group.

To further investigate transfection efficiency, immunofluorescence was performed to identify hIFN- λ 1 and NDV expression in the three groups. hIFN- λ 1-positive cells were stained green, while NDV positive cells were stained red (Fig 1d). NDV expression was increased in the rL-hIFN- λ 1 and NDV groups. Furthermore, A549 cells in the rL-hIFN- λ 1 group displayed dramatic hIFN- λ 1 and NDV expression compared to cells in the NDV group. A549 cells in the PBS group displayed almost no expression of NDV or hIFN- λ 1.

rL-hIFN- λ 1 inhibits A549 cell proliferation and migration

To explore the role of rL-hIFN- λ 1, A549 cells were treated with various concentrations of rL-hIFN- λ 1 or NDV for 24 hours. MTT was used to assess cell viability. As shown in Figure 2a, A549 cell growth was effectively inhibited by rL-hIFN- λ 1 compared to NDV in a dose-dependent manner. Therefore, rL-hIFN- λ 1 at an MOI of 10 was selected for further experiments. In addition, rL-hIFN- λ 1 significantly inhibited the proliferation of A549 cells (Fig 2a).

Figure 1 IL-28R, hIFN- λ 1, and Newcastle disease virus (NDV) expression levels. (a) IL-28R protein expression was detected in A549, SK-MES-1, and Lewis lines by Western blot. (b) hIFN- λ 1 secretion was monitored by enzyme-linked immunosorbent assay. * $P < 0.05$ (rL-hIFN- λ 1 vs. NDV) (▨) NDV, (▩) rL-hIFN- λ 1. hIFN- λ 1 expression in A549 cells was detected by (c) PCR and (d) immunofluorescent staining. Representative immunofluorescence photomicrographs of A549 cells show that hIFN- λ 1 in the rL-hIFN- λ 1 group dramatically increased compared to the NDV and phosphate buffered saline groups.



The properties of inhibition of rL-hIFN- λ 1 on A549 cells were also determined by clonogenic assay. As shown in Figure 2b, rL-hIFN- λ 1 greatly reduced colony formation in the rL-hIFN- λ 1 group compared to the NDV or PBS groups (Fig 2b). An inverted microscope was used to measure the effect of rL-hIFN- λ 1 and NDV on cell growth. We observed that A549 cells infected with rL-hIFN- λ 1 were significantly attenuated and morphologically had shrunk (Fig 2c). Transwell assay was used to determine the migration and invasion of A549 cells treated with rL-hIFN- λ 1. The results revealed that A549 cells infected with rL-hIFN- λ 1 migrated slower than in the NDV and PBS groups (Fig 2d). Consistent with this observation, we further examined the migration ability of A549 cells using scratch migration assay. We further confirmed that A549 cells in the rL-hIFN- λ 1 group exhibited reduced migration compared to the NDV and PBS groups (Fig 2e).

rL-hIFN- λ 1 induces the endoplasmic reticulum stress (ERS) response and apoptosis in A549 cells

To evaluate whether rL-hIFN- λ 1 can induce ERS and apoptosis in lung adenocarcinoma A549 cells, transmission electron microscopy was performed. ERS, apoptosis, and autophagosomes in A549 cells in the rL-hIFN- λ 1 group dramatically increased (Fig 2f). We then measured the expression levels of their related proteins (GRP78, CHOP, p-eIF2 α and beclin1) in A549 cells treated with rL-hIFN- λ 1, NDV, or PBS. GRP78, CHOP, and p-eIF2 α levels were

significantly elevated in the rL-hIFN- λ 1 group compared to the NDV and PBS groups as (Fig 3a). Consistent with these observations, immunofluorescence imaging showed that GRP78 and CHOP were stably expressed at a higher level in the rL-hIFN- λ 1 group compared to the NDV and PBS groups (Fig 3b). Furthermore, the increased ERS response and autophagy markers were affected in time (Fig 3c) and dose dependent manners by rL-hIFN- λ 1 (Fig 3d). We further examined whether rL-hIFN- λ 1 was involved in apoptosis. Western blot showed that the levels of apoptosis-related proteins, such as cleaved caspase3, cleaved caspase8, and cleaved caspase9 were substantially upregulated in the rL-hIFN- λ 1 group, while the level of BCL-2/Bax dramatically decreased (Fig 3e). Flow cytometry confirmed that the application of rL-hIFN- λ 1 for 24 hours dramatically increased apoptosis (Fig 3f).

4-PBA or small interfering RNA (siRNA) knockdown reduced ERS, autophagy, and apoptosis related protein expression

We treated A549 cells with rL-hIFN- λ 1, NDV, or PBS in the presence or absence of 4-PBA, a representative ERS inhibitor. The expression of these ERS (p-eIF2 α and CHOP), apoptosis (cleaved caspase3), and autophagy (LC3II) related proteins were significantly reduced in A549 cells treated with 4-PBA pretreatment (Fig 4a). These observations suggested that the ERS response occurred prior to autophagy and apoptosis.

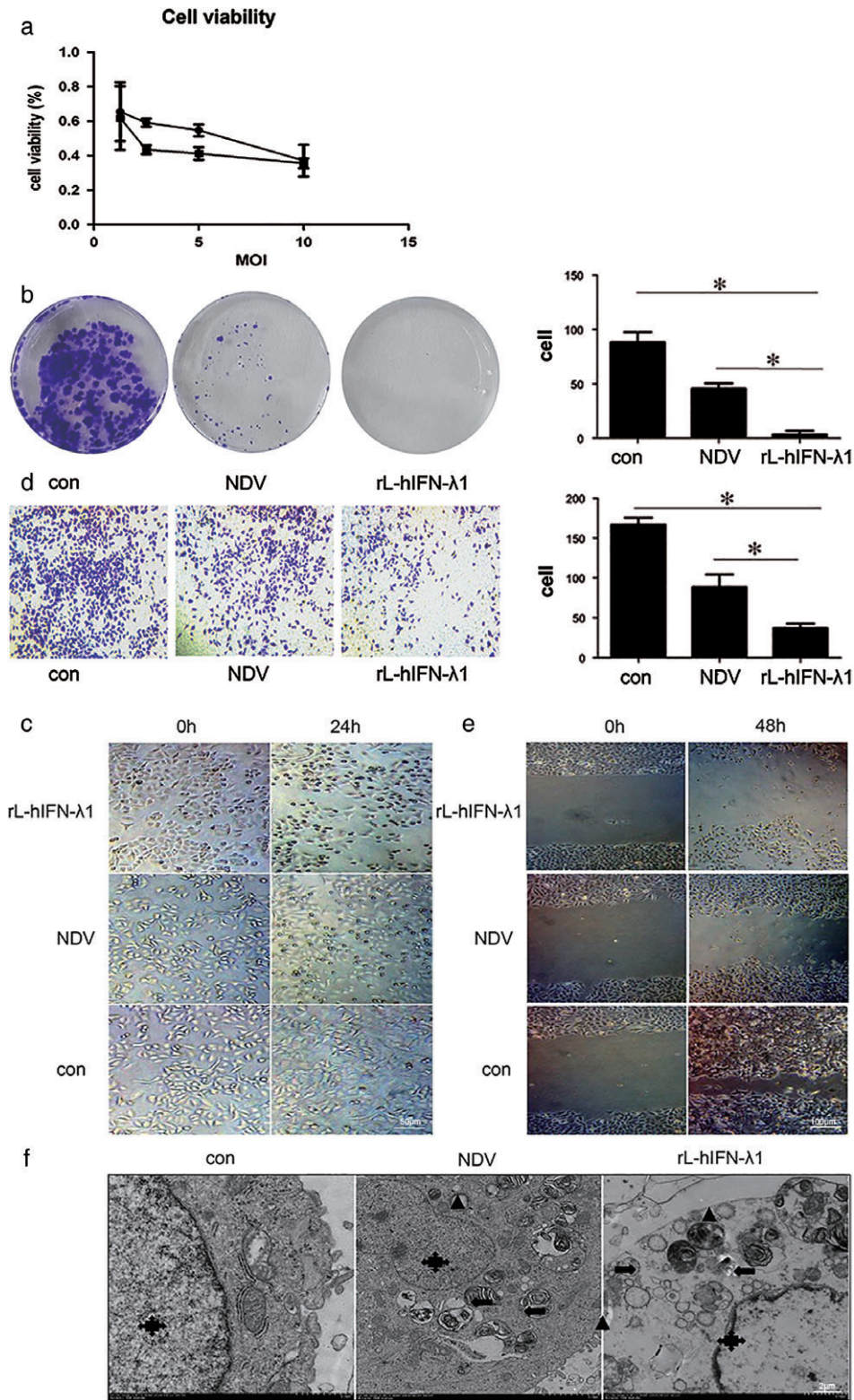
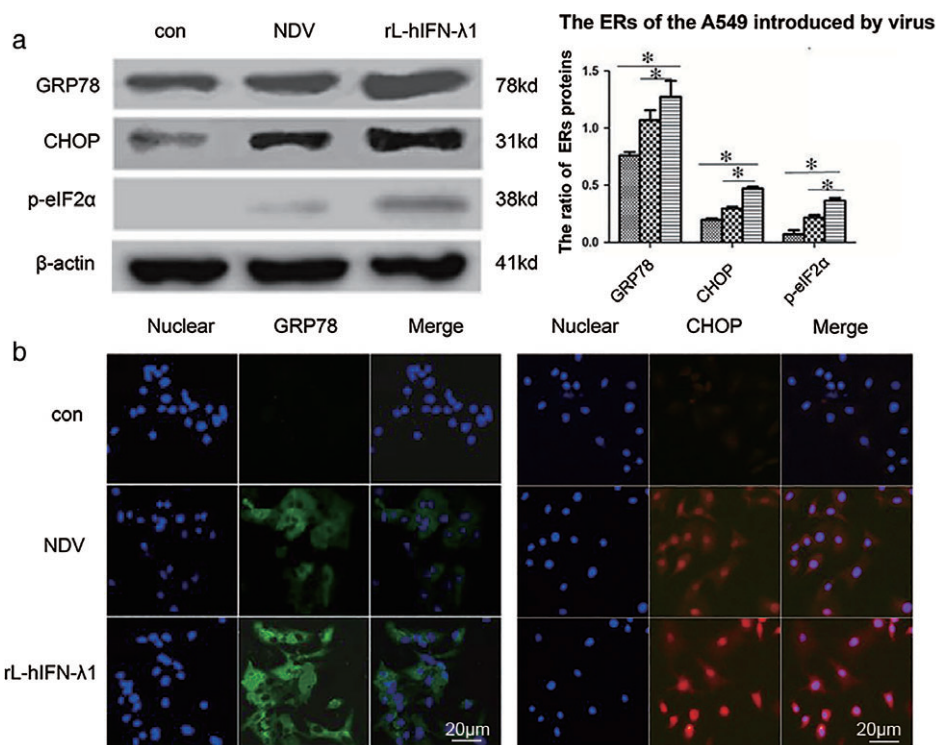


Figure 2 rL-hIFN-λ1 inhibits A549 cell proliferation and migration. (a) A549 cells were treated with rL-hIFN-λ1 and Newcastle disease virus (NDV) for 24 hours and cell viability was quantified by methyl-thiazolyl-tetrazolium assay; **P* < 0.05 (rL-hIFN-λ1 vs. NDV) (●) NDV, (■) rL-hIFN-λ1. (b) The clonogenic activity of A549 cells after treatment with rL-hIFN-λ1 and NDV at a multiplicity of infection of 10. The samples were then incubated in fresh medium for 10 days, and fixed and stained with 0.2% crystal violet. Colony formation was attenuated in the rL-hIFN-λ1 group. **P* < 0.05 (rL-hIFN-λ1 vs. NDV and phosphate buffered saline [PBS] groups, respectively). (c) Representative images of morphological changes of A549 cells were captured (40x magnification). rL-hIFN-λ1 significantly (d) attenuated invasion and (e) inhibited the migration of A549 cells. (f) The ultrastructure of the A549 cells after infection with rL-hIFN-λ1. Arrows indicate the autophagosome, a black triangle indicates the endoplasmic reticulum stress (ERS), and a black star indicates the nucleus. Compared to the NDV and PBS groups, the number of ERS, apoptosis, and autophagosomes in A549 cells in the rL-hIFN-λ1 group was obviously increased.

To confirm whether the ERS response occurred prior to autophagy and apoptosis, CHOP, a downstream component of ERS pathways, was knocked down (the siCHOP

sequences are shown in Table 1). CHOP knockdown efficacy was confirmed by Western blot. As expected, CHOP expression significantly decreased after CHOP knockdown.

Figure 3 rL-hIFN- λ 1 induces the endoplasmic reticulum stress (ERS) response and apoptosis in A549 cells. (a) Western blot was used to detect ERS response-related proteins (▨) con, (▩) Newcastle disease virus (NDV), (≡) rL-hIFN- λ 1. (b) Representative immunofluorescence photomicrographs of GRP78 and CHOP. The expression of ERS-related proteins when A549 cells were treated with rL-hIFN- λ 1 for (c) different time intervals and (d) at different concentrations. (e) Immunoblots show that the expression of ERS markers GRP78, CHOP, and p-eIF2 α , after treatment with rL-hIFN- λ 1 peaked at 24 hours and at a multiplicity of infection (MOI) of 10. Apoptosis proteins were measured by Western blot (▨) con, (▩) NDV, (≡) rL-hIFN- λ 1. Bar graphs show the relative expression level (* P < 0.05; ** P < 0.01). (f) Flow cytometry analysis was used to confirm apoptotic cells (* P < 0.05). Apoptosis in A549 cells was increased with rL-hIFN- λ 1.



Furthermore, apoptosis and autophagy related proteins, such as caspase3 and LC3II, were obviously downregulated (Fig 4b). This result showed that blocking ERS significantly reduced apoptosis and autophagy.

The ERS pathway consists of three primary pathway proteins: PERK, ATF6, and IRE-1. The PERK-CHOP pathway is the most important. The PERK pathway includes the phosphorylation of eIF2 α and CHOP.¹⁵ We investigated whether ERS caused autophagy or apoptosis via immunoblotting. Blocking of PERK by siRNA (the siPERK sequences are shown in Table 1) resulted in a significant decrease in p-PERK, p-eIF2 α , CHOP, caspase3, and LC3II, which were induced by rL-hIFN- λ 1 or NDV, suggesting that the ERS response induced autophagy and apoptosis (Fig 4c).

JNK inhibitor reduced autophagy and apoptosis protein expression

JNK is a downstream sensor of IRE1 that can activate both IRE1-XBP-1-CHOP (an ERS-associated pathway) and TRAF2/JNK pathways. Evidence has revealed that IRE1 promotes the caspase pathway by activating JNK.¹⁶ Studies have revealed that JNK is involved in inducing autophagy through BCL-2 phosphorylation and disruption of the BCL-2/beclin1 complex.¹⁷ The data suggests that JNK

activation may be associated with autophagy and apoptosis induction. To investigate whether JNK is involved in the regulation of autophagy and apoptosis related proteins, ERS, autophagy, and apoptosis related protein expression levels were evaluated by Western blot in A549 cells treated with rL-hIFN- λ 1 or NDV in the absence or presence of the JNK inhibitor SP600125. As shown in Figure 5, p-JNK was significantly attenuated in the presence of the JNK inhibitor. Caspase3 and LC3II expression decreased in the presence of the JNK inhibitor, while BCL-2 increased.

BCL-2 depletion with siRNA increases rL-hIFN- λ 1-induced autophagy and apoptosis

The BCL-2 protein family plays a key role in regulating apoptosis and autophagy.^{18–20} To determine BCL-2 knock-down efficacy, FAM-siRNA of BCL-2 (sequences of siBCL-2 shown in Table 1) was utilized, according to the instructions (Fig 6a). Green fluorescence limited to membrane indicated that BCL-2 was knocked down. Growth was then measured using clonal clusters stained with crystal violet (Fig 6b). Intriguingly, we observed that when BCL-2 was knocked down by siRNA, the colony formation numbers of A549 infected with rL-hIFN- λ 1 were markedly reduced compared to those treated with NDV or PBS.

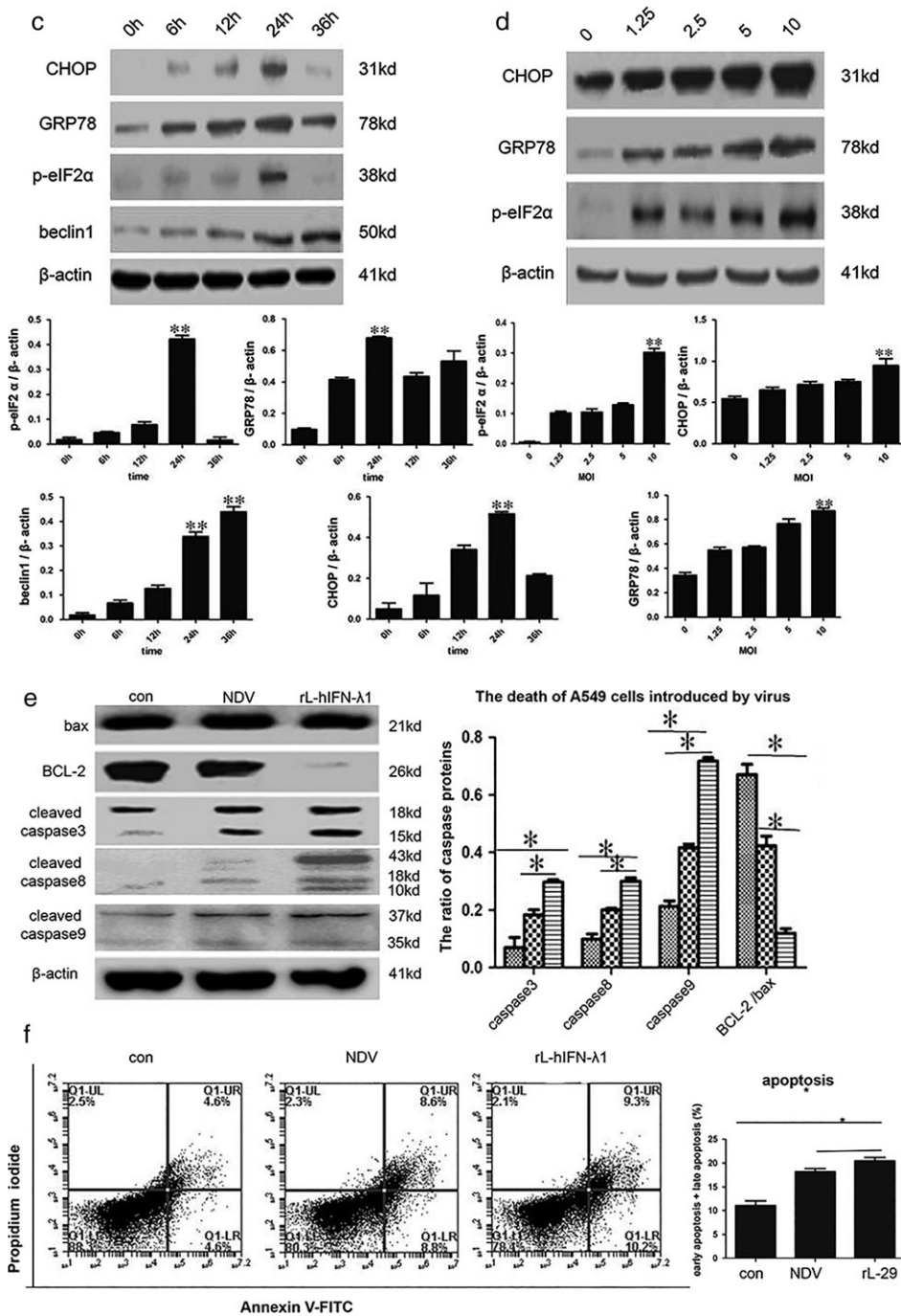


Figure 3 (Continued)

To gain further insight into the mechanism by which BCL-2 siRNA exacerbated autophagy and apoptosis in A549 cells, Western blot was used to detect several proteins involved in autophagy (LC3I-LC3II and beclin1), apoptosis (caspase3), and anti-apoptosis (BCL-2). We found that the presence of BCL-2 siRNA resulted in a significant increase in the expression of LC3II, beclin1, and caspase3, a decrease in BCL-2 expression, and knockdown of BCL-2 when A549 cells were treated with rL-hIFN-λ1, NDV, or

PBS for 24 hours (Fig 6c). These findings indicate that BCL-2 knockdown induces autophagy and apoptosis.

rL-hIFN-λ1 inhibits subcutaneous growth of A549 cells and induces natural killer cell increases in vivo

We used a tumor-bearing mouse model to determine whether rL-hIFN-λ1 exerted an antitumor effect in vivo

Figure 4 4-PBA or knockdown using small interfering RNA (siRNA) reduced the expression of endoplasmic reticulum stress (ERS), apoptosis, and autophagy related proteins. (a) Effects of 4-PBA on A549 cells treated with rL-hIFN-λ1, Newcastle disease virus (NDV), and phosphate buffered saline (PBS) (con), 4-PBA. (b) Expression of CHOP, LC3-I to LC3-II conversion, and caspase3 in the siCHOP-transfected A549 cells (con), siCHOP. (c) Expression of p-PERK, p-eIF2α, CHOP, LC3II, and caspase3 in A549 cells transfected with siPERK (con), siPERK (**P* < 0.05). Immunoblot shows that the expression of ERS, autophagy, and apoptosis markers p-PERK, p-eIFα, CHOP, LC3II, and caspase3 decreased after ERS was blocked.

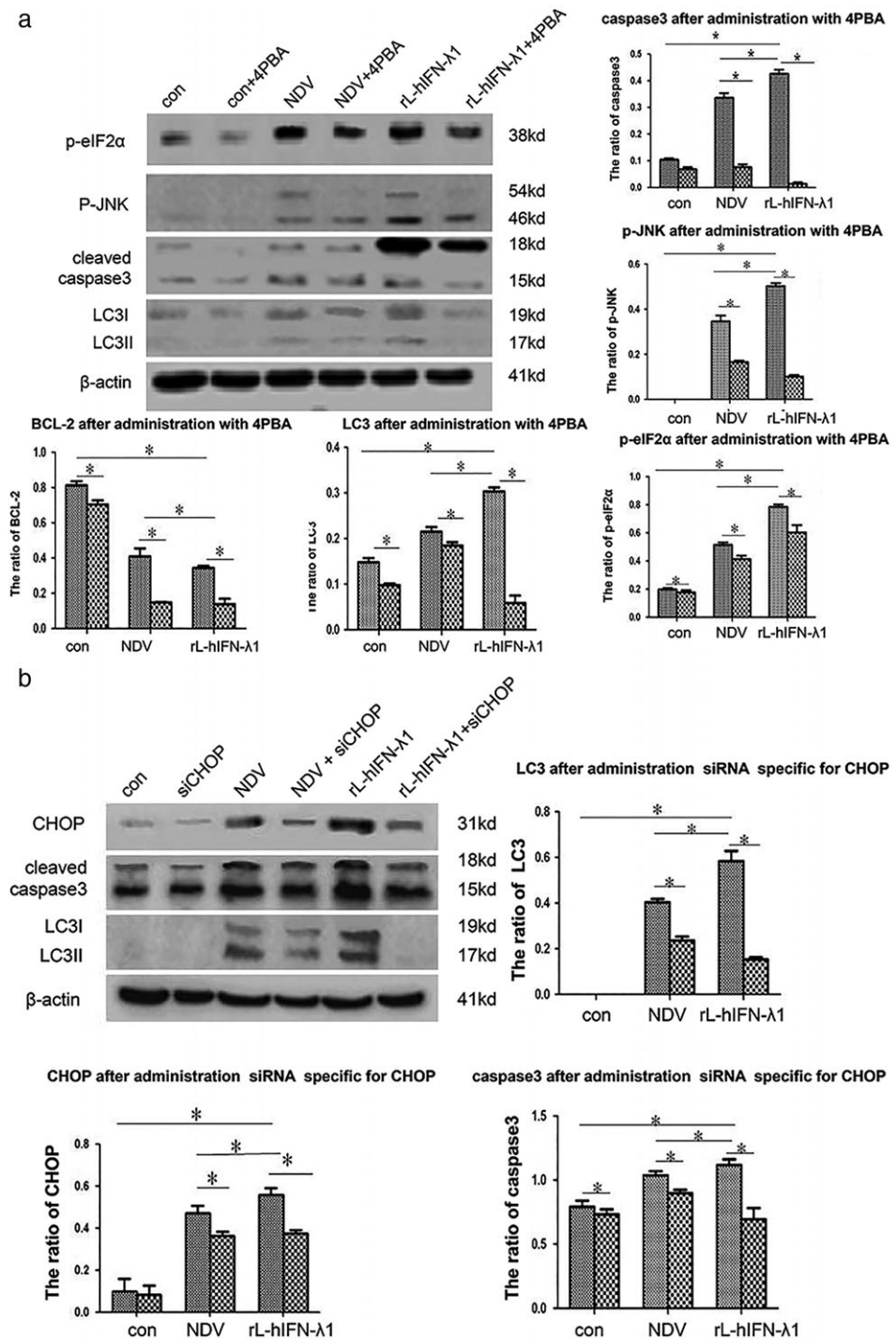


(Fig 7a). The tumor volumes of nude mice treated with rL-hIFN-λ1 were significantly reduced compared to those in the NDV or PBS groups (Fig 7b).

After hematoxylin and eosin staining, the tumors in the rL-hIFN-λ1 and NDV groups demonstrated a typical histological pattern characterized by severe necrotic tumor cells, which was not observed in the PBS group. In addition, cell

necrosis dramatically increased in the rL-hIFN-λ1 group (Fig 7c).

The number of NK cells was confirmed by flow cytometry. Consistent with the previous result, the number of NK cells was dramatically increased in the rL-hIFN-λ1 group compared to the PBS and NDV groups (*P* < 0.05) (Fig 7d). IFN-λs are reported to play a critical role in modulating

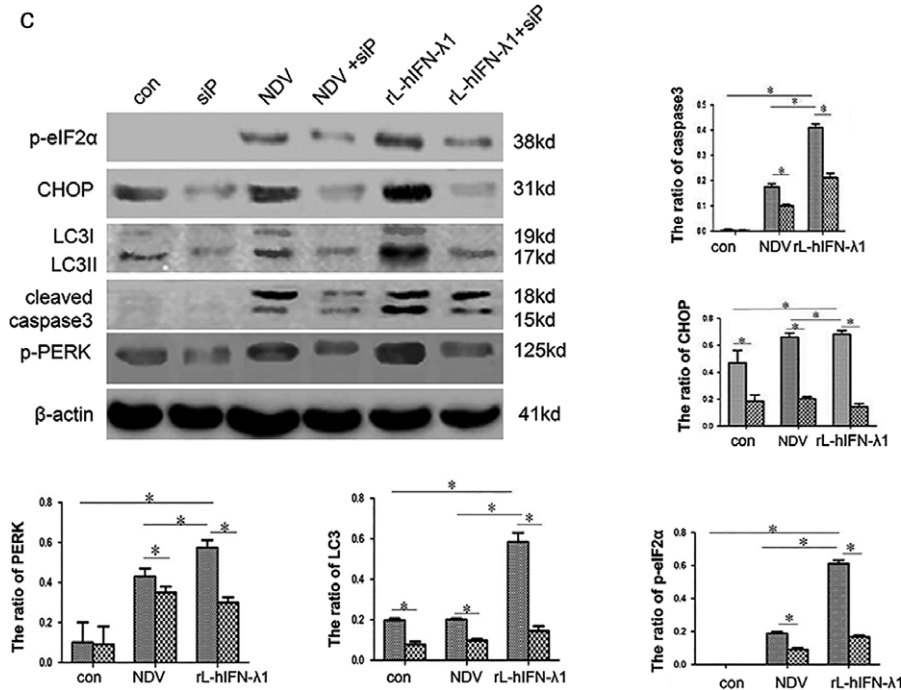


Figure 4 (Continued)

the immune system, similar to the roles played by type I IFN-λs and NK cells, and are increased in the spleen blood in cells treated with r-Ad-hIFN-λ1.²¹ These results demonstrated that rL-hIFN-λ1 induces potent suppression of tumor growth and activates the immune system.

Efficiency of hIFN-λ1 infection to induce ERS response and apoptosis in vivo

Expression of hIFN-λ1 and NDV proteins in tumor tissues

Western blot analysis was used to determine the expression of hIFN-λ1 and NDV proteins in tumor tissues. hIFN-λ1 was dramatically increased in the rL-hIFN-λ1 group, whereas in the PBS and NDV groups it was significantly reduced. On the other hand, NDV was expressed in both rL-hIFN-λ1 and NDV groups, but not in the PBS group (Fig 8a).

Immunohistochemistry was performed to identify NDV and hIFN-λ1 protein expression in tumor tissues. We observed that NDV expression in the NDV and rL-hIFN-λ1 groups was higher in tumor tissues than in the PBS group. Next, we assessed the expression and localization of hIFN-λ1 in tumor tissues via immunohistochemical analysis. hIFN-λ1 was strongly expressed in the rL-hIFN-λ1 group compared to the NDV group, and was not expressed in the PBS group (Fig 8b). These findings demonstrated that both rL-hIFN-λ1 and NDV successfully infected A549 cells in vivo.

ERS response and apoptosis induced by rL-hIFN-λ1 in tumor specimens

One mechanism to induce apoptosis is via ERS.¹¹ rL-hIFN-λ1 infection of A549 cells was examined to identify unfolded protein response (UPR) marker expression in vitro. Additional analysis was performed on ERS-related proteins in tumor specimens. To detect ERS, autophagy, and apoptosis markers in tumor tissues, we measured the expression levels of GRP78, CHOP, p-eIF2α, beclin1, LC3, and caspase3 in tumor specimens obtained from tumor-bearing mice treated with rL-hIFN-λ1, NDV, or PBS. ERS, autophagy, and apoptosis related proteins were upregulated in tumor specimens from the rL-hIFN-λ1 group compared to specimens from the NDV and PBS groups (Fig 8c).

Discussion

Despite improvements in the detection and treatment of early-stage lung cancer, which may be a result of the increased use of computed tomography (CT), a third of patients with early-stage lung cancer survive less than five years.^{22–25} This is partially attributable to the limited therapeutic efficacy of surgery, radiation, and chemotherapy in lung cancer. Fortunately, accumulating evidence has revealed the significant role of oncolytic tumor therapy.^{26–28}

Newcastle disease virus is reported to be a safe and effective oncolytic therapeutic agent for lung cancer.²⁹ NDV has been used to treat neuroblastoma, melanoma, and other malignancies. Previous studies have reported that the

Table 1 siRNA sequences used for knockdown

Gene Name	Sequence	
	Sense (5'-3')	Antisense (5'-3')
siRNA (CHOP-HOMO-805)	GAGCUCUGAUUGACCGAAUTT	AUUCGGUCAAUACAGAGCUCTT
siRNA (PERK-HOMO-2370)	GGAUGCACCAUCAGUAAAATT	UUUAAACUGAUGGUGCAUCCTT
siRNA (BCL2-HOMO-506)	GGGAGAACAGGGUACGAUATT	UAUCGUACCCUGUUCUCCTT

siRNA, small interfering RNA.

tumor volume is substantially decreased after NDV infection.²⁹⁻³¹

Interferons have multiple functions, including anti-tumor effects and antiviral, immunomodulatory, and anti-proliferative activity.³²⁻³⁴ Previous reports have shown that IFN-λ1 inhibits growth in several tumor cells, such as neuroendocrine tumors, glioblastomas, and colon cancer cell lines.³⁵ The inhibitory effect of r-Ad-hIFN-λ1 on human gastric cancer cells has been validated.²¹ It has been reported that NK cells in the splenic blood increased in an

r-Ad-hIFN-λ1 group as a result of immunomodulatory effects.²¹ In our study, we also observed that NK cells in splenic blood from the rL-hIFN-λ1 group were increased. We speculated that the immune system may play important functions in rL-hIFN-λ1-induced inhibition of tumor formation. Type III IFN is sensed through a compound receptor consisting of IL-10Rb and IL-28R. The levels of IL-28R and IL-10Rb expression were evaluated in A549 cells. hIFN-λ1 may have a higher affinity for IL-28R than IL-28.^{13,14} Our results are consistent with previous results

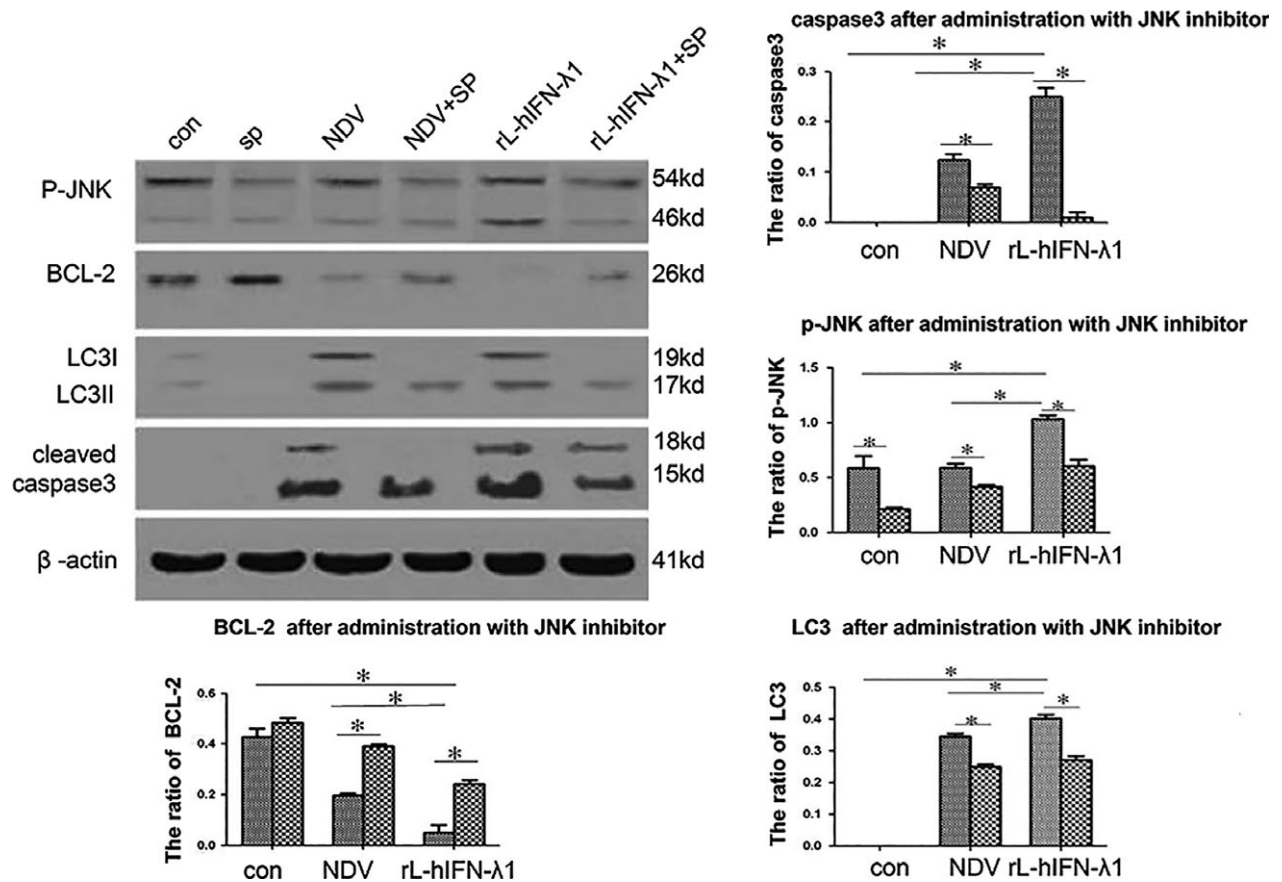


Figure 5 JNK inhibitors reduced the expression of apoptosis and autophagy related proteins. A549 cells pretreated with a JNK inhibitor were then treated with rL-hIFN-λ1, Newcastle disease virus (NDV), or phosphate buffered saline (PBS) for another 24 hours. The effects of JNK inhibitor on the protein levels of p-JNK, BCL-2, LC3 conversion, and cleaved caspase3 were determined by Western blot (**P* < 0.05). (▨) con, (▩) JNK inhibitor. Note the decrease in p-JNK, LC3 conversion, and cleaved caspase3 levels and the increase in the BCL-2 level induced by rL-hIFN-λ1-infected A549 cells after JNK inhibitor administration.

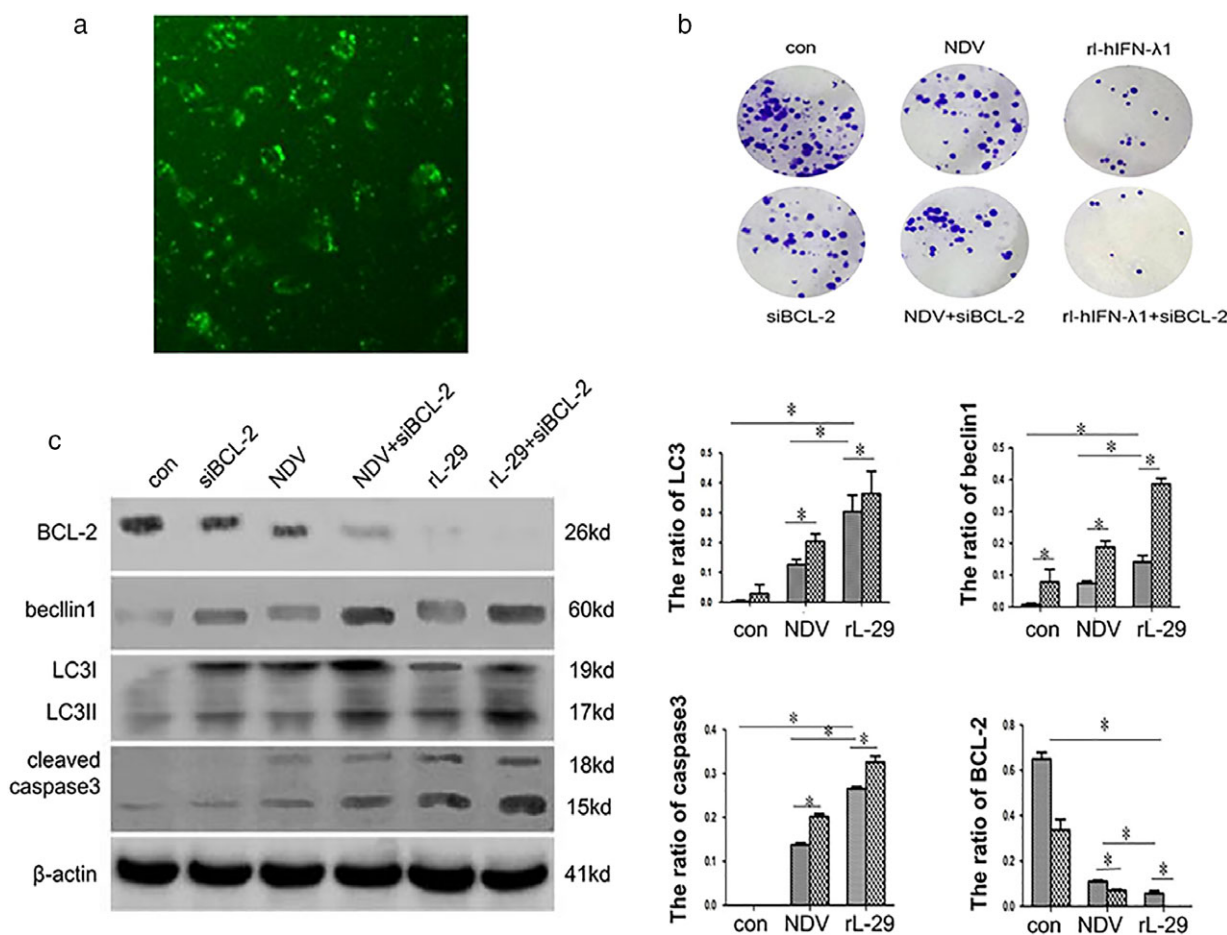


Figure 6 BCL-2 small interfering RNA (siRNA) aggravated A549 cellular apoptosis and autophagy. (a) The transfection efficiency of knockdown of BCL-2 in A549 cells. (b) Colony-formation assays were used to measure the colony formation capability of A549 cells with BCL-2 knockdown. (c) Representative Western blot and quantitative analysis of apoptosis markers (caspase3) and autophagy markers (LC3 conversion and beclin1) in A549 cells with or without BCL-2 siRNA followed by rL-hIFN- λ 1, Newcastle disease virus (NDV), and phosphate buffered saline (PBS). The expression of LC3 conversion, beclin1, and caspase3 obviously increased when BCL-2 was knocked down (* $P < 0.05$). (▨) con, (▩) siBCL-2.

indicating that IL-28R is expressed in A549 cells. We further investigated the role and underlying mechanisms of rL-hIFN- λ 1 in A549 cells.

Immunofluorescence showed that hIFN- λ 1 and NDV were expressed in the A549 cell cytoplasm in the rL-hIFN- λ 1 group. We also examined hIFN- λ 1 secretion from the supernatants of rL-hIFN- λ 1-infecting cells with ELISA and found that secreted hIFN- λ 1 was significantly higher in the rL-hIFN- λ 1 than in the NDV group. rL-hIFN- λ 1 could infect A549 cells with high efficiency and hIFN- λ 1 cytokines were produced. Consistent with the results of cell experiments, Western blot and tumor tissue immunohistochemistry revealed that hIFN- λ 1 was highly expressed in the rL-hIFN- λ 1 group compared to the NDV and PBS groups. We hypothesized that hIFN- λ 1 interacted with the receptor on A549 cells and then aggravated cell death.

To elucidate the role of rL-hIFN- λ 1 in A549 cells, MTT and clonogenic assays, and an inverted microscope were

used to observe the A549 cells exposed to rL-hIFN- λ 1, which were inclined to undergo cell death compared to exposure to NDV or PBS. These results indicate that rL-hIFN- λ 1 plays an important role in the growth of A549 cells. Moreover, transmission electron microscopy showed that the numbers of ERS, apoptotic cells, and autophagosomes were substantially increased in rL-hIFN- λ 1-infected A549 cells. Thus, the underlying mechanisms among rL-hIFN- λ 1-induced death, ERS, and autophagy in A549 require further investigation.

Recently, increasing evidence has revealed that ERS is involved in lung cancer in vivo and in vitro. ERS occurs in several diseases, including cancer.³⁶ Following ERS, the UPR is activated to alleviate ERS. The UPR consists of three primary branches of signaling pathways with three distinct stress sensors, including PERK, ATF6, and IRE1.³⁷ Once ERS occurs, the hallmark of the UPR is to upregulate some factors, including GRP-78 and CHOP.³⁸ The PERK

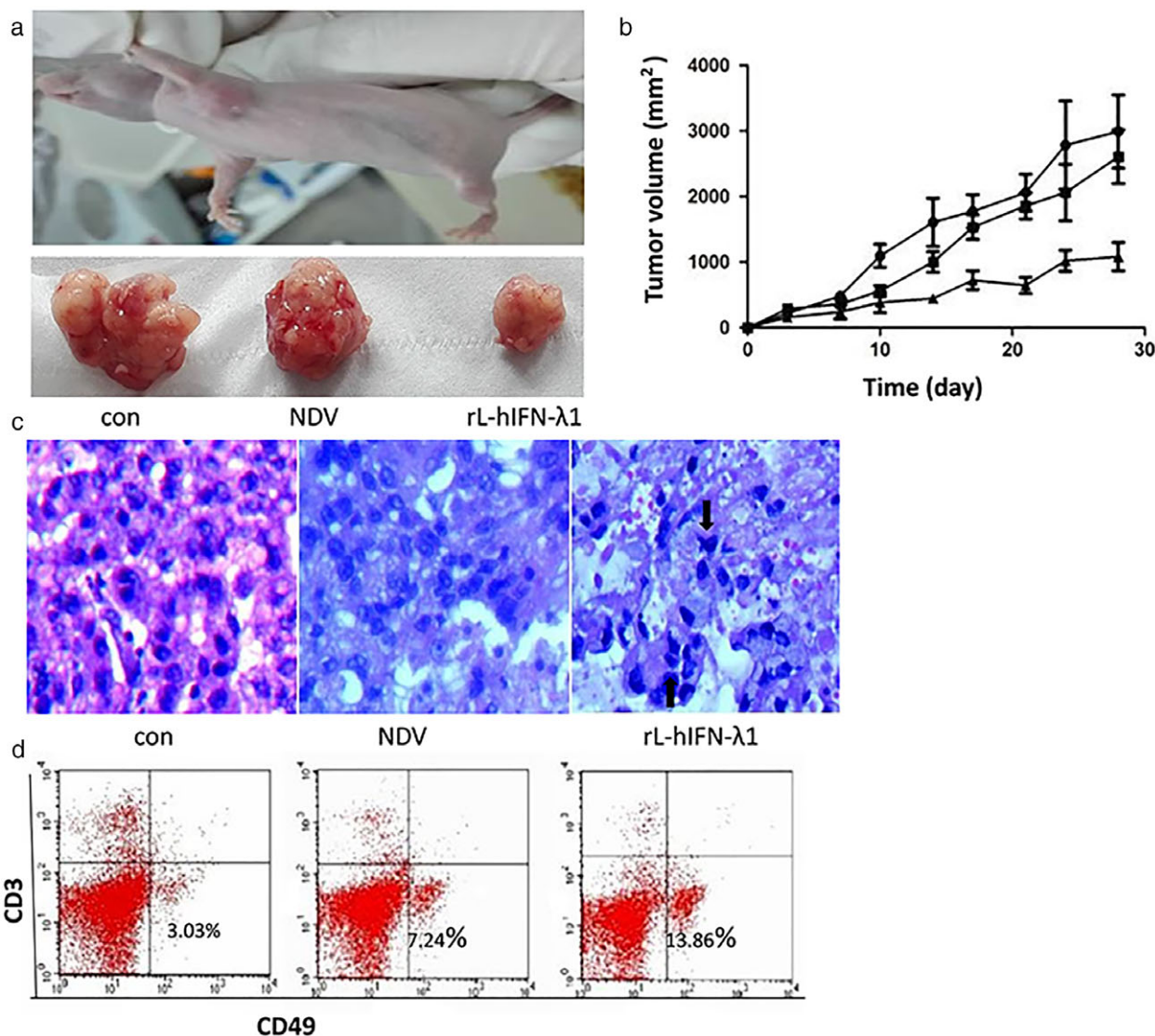


Figure 7 rL-hIFN- λ 1 inhibits subcutaneous growth of A549 cells and induces an increase in natural killer (NK) cells. (a) Images of tumors formed by A549 cells. (b) The growth curves of the tumors in the rL-hIFN- λ 1, Newcastle disease virus (NDV), and phosphate buffered saline (PBS) groups (—●—) con, (—■—) NDV, (—▲—) rL-hIFN- λ 1. The effect of rL-hIFN- λ 1 on histopathological changes in tumor tissues after a tumor-bearing mouse model was injected with different viruses. (c) Histologic outcomes of hematoxylin and eosin staining. The arrows indicate necrotic cells. (d) The number of NK cells in the spleen after a tumor-bearing mouse model was injected with rL-hIFN- λ 1, NDV, and PBS (* $P < 0.05$).

signaling pathway plays a key role in ERS,^{15,17} therefore, we explored the PERK-CHOP signaling pathway. We found that GRP78, p-eIF2 α , CHOP, and the levels of other UPR-related markers were substantially increased in A549 cells and lung tissues in the tumor-bearing mice treated with rL-hIFN- λ 1. Consistent with this observation, cleaved caspase3, cleaved caspase8, and cleaved caspase9 were also significantly increased in A549 cells in the rL-hIFN- λ 1 group. As supporting data, we found that cleaved caspase3, beclin1, and LC3II were markedly up-regulated in tumor tissues in the rL-hIFN- λ 1 group. These

findings imply that rL-hIFN- λ 1 is involved in the induction of ERS, autophagy, and apoptosis in lung adenocarcinoma A549 cells.

Some scholars have posited that severe ERS precedes autophagy and apoptosis in glioma cells.³⁹ We found that following the administration of 4-PBA, p-eIF2 α and p-JNK activity was partially inhibited. At the same time, the expression of caspase3 and LC3II conversion decreased. Intriguingly, ERS protein levels were substantially decreased by both the administration of the ERS inhibitor 4-PBA and treatment with siPERK.

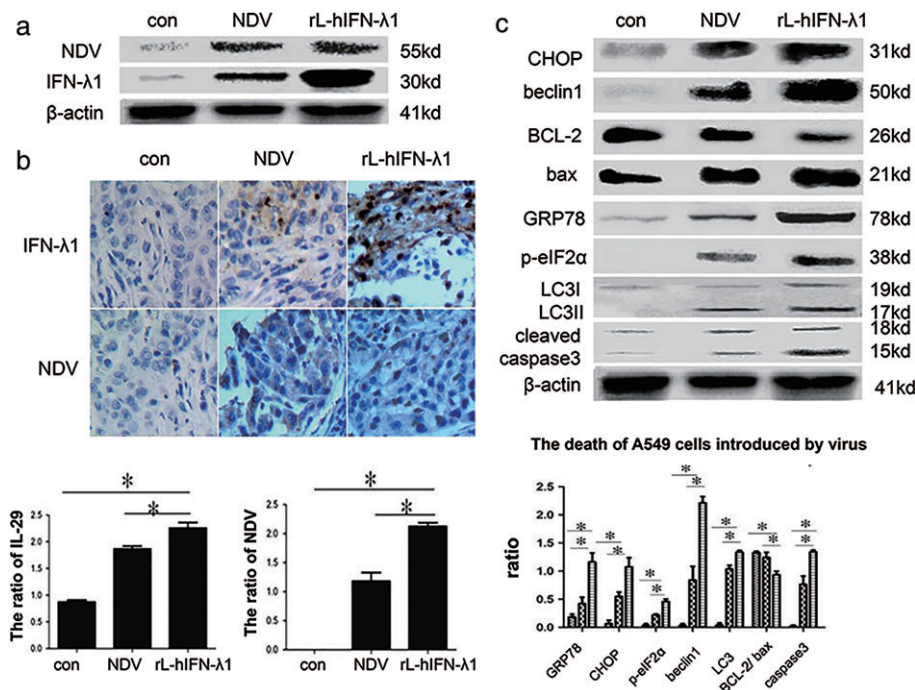


Figure 8 Transfection efficiency of hIFN- λ 1 in tumor tissues and endoplasmic reticulum stress (ERS), autophagy, and apoptosis induced by rL-hIFN- λ 1 in tumor specimens with A549 cells. hIFN- λ 1 and Newcastle disease virus (NDV) protein expression in tumor tissues were determined by (a) Western blot and (b) immunohistochemistry (magnification 400 \times). (c) The expression of ERS, autophagy, and apoptosis-associated makers induced by rL-hIFN- λ 1 in tumor specimens of A549 cells ($*P < 0.05$). (▨) con, (▩) NDV, (▧) rL-hIFN- λ 1. Immunoblot shows the increased levels of GRP78, CHOP, p-eIF2 α , beclin1, LC3 conversion, and cleaved caspase3 and decrease of BCL-2/Bax in tumor specimens with A549 cells. Note the increase in ERS, autophagy, and apoptosis hallmarks in rL-hIFN- λ 1-treated tumor specimens.

CHOP, a downstream component of ERS pathways at the convergence of the IRE1, PERK, and ATF6 pathways, is a pro-apoptotic mediator.⁴⁰ Several reports have suggested that CHOP accumulation is responsible for ERS-induced apoptosis.^{17,41,42} In our study, LC3-II conversion and caspase3 substantially decreased after transfection with siCHOP, which implies that rL-hIFN- λ 1-induced ERS is responsible for autophagy and apoptosis in A549 cells.

PERK, a Ser/Thr protein kinase, induces apoptosis.³⁹ Once ERS occurs, it stimulates PERK phosphorylation. Activated PERK then phosphorylates eIF2 α . As a result, PERK signaling protects the cell from protein misfolding in the ER.⁴³ On the other hand, CHOP is located downstream of the PERK-CHOP pathway and damages the cell. Our findings show that A549 cells treated with rL-hIFN- λ 1 activate the PERK-eIF2 α pathway and induce CHOP expression, consistent with the results of previous studies. We observed that the PERK blockade also decreased p-PERK, p-eIF α , CHOP, LC3II, and caspase3 expression. Collectively, these results indicate that rL-hIFN- λ 1 could mediate autophagy and apoptosis via the PERK-CHOP signaling pathway in the lung cancer A549 cell line.

The IRE1 α -ASK1-JNK signaling pathway also plays critical functions in cell death. Activation of JNK1 leads to BCL-2 phosphorylation, dissociates BCL-2 from beclin1, and induces autophagy during normal growth conditions.¹⁸ Previous studies have reported that the JNK-mediated degradation of BCL-2 stimulates autophagy.¹⁹ The inhibition of JNK significantly suppresses autophagy.¹⁷ Studies have

indicated that BCL-2 phosphorylation may represent a mechanism for regulating both autophagy and apoptosis.²⁰ We found that pretreatment with the JNK inhibitor SP600125 could attenuate p-JNK and increase BCL-2 induction by rL-hIFN- λ 1. Moreover, inhibition of JNK abrogated rL-hIFN- λ 1-induced accumulation of LC3-II and caspase3 in A549 cells. These results are consistent with the findings of previous studies. JNK phosphorylation is also reported to activate the pro-apoptotic BCL-2 family member BIM.⁴³ When BCL-2 phosphorylation reaches maximal levels, such as after prolonged starvation, the BCL-2-Bax complex is disrupted and caspase3 is activated, which indicates the initiation of apoptosis.¹⁸ In addition, prolonged JNK1 activation can mediate apoptosis.¹⁸ Yoo *et al.* suggested that BCL-2 has anti-apoptotic and anti-autophagic functions.¹⁸ The BCL-2 inhibitor ABT263 delays the onset of tumor formation in mice, thus selective BCL-2 inhibition using RNA interference causes an apoptotic response in cells.⁴⁴ To further clarify whether rL-hIFN- λ 1-induced cell death was related to the IRE1 α -ASK1-JNK signaling pathway, BCL-2 siRNA was used to knock down BCL-2 to elucidate the effect of BCL-2 on autophagy and apoptosis. Our results indicated that BCL-2 knockdown inhibits BCL-2 activity. The expression of beclin1 and LC3II, two autophagy markers, was increased in parallel with the expression of apoptosis marker caspase3. Collectively, these findings indicate that BCL-2 plays a key role in anti-apoptosis and anti-autophagy, and rL-hIFN- λ 1 induces apoptosis in part through the IRE1-JNK-BCL-2 pathway in A549 cells.

In summary, we found that rL-hIFN- λ 1-induced death may occur through the immune system and via ERS-induced autophagy and apoptosis. Inhibition of the ERS pathway could further decrease autophagy and apoptosis induced by rL-hIFN- λ 1. rL-hIFN- λ 1-induced ERS may play an important role in autophagy and apoptosis in human lung cancer A549 cells. During this process, the PERK-CHOP and IRE1-JNK pathways played a major role. Therefore, our data suggest that rL-hIFN- λ 1 may be a powerful candidate for antitumor treatments.

Acknowledgments

We thank Zhijian Zhang for excellent experimental assistance, and the Key Laboratory of Veterinary Biotechnology, Harbin Veterinary Research Institute, Chinese Academy of Agricultural Sciences for kindly helping to construct rL-hIFN- λ 1. This work was supported by grants from the Project of Natural Science Foundation of Jiangsu Province, China (BK20151333) and the National Natural Science Foundation of China (81672999).

Disclosure

No authors report any conflict of interest.

References

- Bray F, Jemal A, Grey N, Ferlay J, Forman D. Global cancer transitions according to the Human Development Index (2008–2030): A population-based study. *Lancet Oncol* 2012; **13**: 790–801.
- Song X, Shi K, Zhou SJ *et al.* Clinicopathological significance and a potential drugtarget of RAR β in non-small-cell lung carcinoma: A meta-analysis and a systematic review. *Drug Des Devel Ther* 2016; **10**: 1345–54.
- Pal S, Amin PJ, Sainis KB, Shankar BS. Potential Role of TRAIL in metastasis of mutant KRAS expressing lung adenocarcinoma. *Cancer Microenviron* 2016; **9**: 77–84.
- Yarchoan M, Lim M, Brahmer JR *et al.* Oligometastatic adenocarcinoma of the lung: A therapeutic opportunity for long-term survival. *Cureus* 2015; **7**: e409.
- Xu P, Zhao M, Liu Z *et al.* Elevated nuclear CCND1 expression confers an unfavorable prognosis for early stage lung adenocarcinoma patients. *Int J Clin Exp Pathol* 2015; **8**: 15887–94.
- Elankumaran S, Chavan V, Qiao D *et al.* Type I interferon-sensitive recombinant Newcastle disease virus for oncolytic virotherapy. *J Virol* 2010; **84**: 3835–44.
- Vigil A, Park MS, Martinez O *et al.* Use of reverse genetics to enhance the oncolytic properties of Newcastle disease virus. *Cancer Res* 2007; **67**: 8285–92.
- Dusheiko G. Side effects of alpha interferon in chronic hepatitis C. *Hepatology* 1997; **26**(3 Suppl 1): 112S–21S.
- Kotenko SV, Gallagher G, Baurin VV *et al.* IFN-lambdas mediate antiviral protection through a distinct class II cytokine receptor complex. *Nat Immunol* 2003; **4**: 69–77.
- Donnelly RP, Kotenko SV. Interferon-lambda: A new addition to an old family. *J Interferon Cytokine Res* 2010; **30**: 555–64.
- Bu X, Zhao Y, Zhang Z, Wang M, Li M, Yan Y. Recombinant Newcastle disease virus (rL-RVG) triggers autophagy and apoptosis in gastric carcinoma cells by inducing ER stress. *Am J Cancer Res* 2016; **6**: 924–36.
- Bu X, Li M, Zhao Y *et al.* Genetically engineered Newcastle disease virus expressing human interferon- λ 1 induces apoptosis in gastric adenocarcinoma cells and modulates the Th1/Th2 immune response. *ONCOL Rep* 2016; **36**: 1393–402.
- Fujie H, Tanaka T, Tagawa M *et al.* Antitumor activity of type III interferon alone or in combination with type I interferon against human non-small cell lung cancer. *Cancer Sci* 2011; **102**: 1977–90.
- Planet PJ, Parker D, Cohen TS *et al.* Lambda interferon restructures the nasal microbiome and increases susceptibility to Staphylococcus aureus superinfection. *MBio* 2016; **7**: e01939–2015.
- He L, Yuan J, Xu Q *et al.* miRNA-1283 regulates the PERK/ATF4 pathway in vascular injury by targeting ATF4. *PLoS One* 2016; **11**: e0159171.
- Fujimoto A, Kawana K, Taguchi A *et al.* Inhibition of endoplasmic reticulum (ER) stress sensors sensitizes cancer stem-like cells to ER stress-mediated apoptosis. *Oncotarget* 2016; **7**: 51854–64.
- Liu GY, Jiang XX, Zhu X *et al.* ROS activates JNK-mediated autophagy to counteract apoptosis in mouse mesenchymal stem cells in vitro. *Acta Pharmacol Sin* 2015; **36**: 1473–9.
- Yoo YM, Han TY, Kim HS. Melatonin suppresses autophagy induced by clinostat in preosteoblast MC3T3-E1 cells. *Int J Mol Sci* 2016; **17**: 526.
- Levine B, Sinha S, Kroemer G. Bcl-2 family members: Dual regulators of apoptosis and autophagy. *Autophagy* 2008; **4**: 600–6.
- Zhou F, Yang Y, Xing D. Bcl-2 and Bcl-xL play important roles in the crosstalk between autophagy and apoptosis. *FEBS J* 2011; **278**: 403–13.
- Bu XF, Zhang J, Jia LJ *et al.* Effect of human interferon- λ 1 recombinant adenovirus on a gastric cancer orthotopic transplantation model. *Exp Ther Med* 2014; **8**: 1115–22.
- Yu Y, Ding Z, Jian H, Shen L, Zhu L, Lu S. Prognostic value of MMP9 activity level in resected stage I B lung adenocarcinoma. *Cancer Med* 2016; **5**: 2323–31.
- Fujisawa T, Iizasa T, Saitoh Y *et al.* Smoking before surgery predicts poor long-term survival in patients with stage I non-small-cell lung carcinomas. *J Clin Oncol* 1999; **17**: 2086–91.
- Martini N, Bains MS, Bur ME *et al.* Incidence of local recurrence and second primary tumors in resected stage I lung cancer. *J Thorac Cardiovasc Surg* 1995; **109**: 120–9.

- 25 Nesbitt JC, Putnam JB Jr, Walsh GL, Roth JA, Mountain CF. Survival in early-stage non-small cell lung cancer. *Ann Thorac Surg* 1995; **60**: 466–72.
- 26 Huang F, Wang BR, Wu YQ, Wang FC, Zhang J, Wang YG. Oncolytic viruses against cancer stem cells: A promising approach for gastrointestinal cancer. *World J Gastroenterol* 2016; **22**: 7999–8009.
- 27 Wang J, Arulanandam R, Wassenaar R *et al.* Enhancing expression of functional human sodium iodide symporter and somatostatin receptor in recombinant oncolytic vaccinia virus for in vivo imaging of tumors. *J Nucl Med* 2017; **58**: 221–7.
- 28 Rehman H, Silk AW, Kane MP, Kaufman HL. Into the clinic: Talimogene laherparepvec (T-VEC), a first-in-class intratumoral oncolytic viral therapy. *J Immunother Cancer* 2016; **4**: 53.
- 29 Yan Y, Jia L, Zhang J, Liu Y, Bu X. Effect of recombinant Newcastle disease virus transfection on lung adenocarcinoma A549 cells in vivo. *Oncol Lett* 2014; **8**: 2569–76.
- 30 An Y, Liu T, He J *et al.* Recombinant Newcastle disease virus expressing P53 demonstrates promising antitumor efficiency in hepatoma model. *J Biomed Sci* 2016; **23**: 55.
- 31 Chai Z, Zhang P, Fu F *et al.* Oncolytic therapy of a recombinant Newcastle disease virus D90 strain for lung cancer. *Virology* 2014; **11**: 84.
- 32 Lin M, Yu HP. Dexamethasone decreases IL-29 expression in house dust mite-stimulated human bronchial epithelial cells. *J Huazhong Univ Sci Technolog Med Sci* 2015; **35**: 823–7.
- 33 Sato A, Ohtsuki M, Hata M, Kobayashi E, Murakami T. Antitumor activity of IFN- λ in murine tumor models. *J Immunol* 2006; **176**: 7686–94.
- 34 Gough L, Schulz O, Sewell HF, Shakib F. The cysteine protease activity of the major dust mite allergen Der p 1 selectively enhances the immunoglobulin E antibody response. *J Exp Med* 1999; **190**: 1897–902.
- 35 Li Q, Kawamura K, Okamoto S *et al.* Adenovirus-mediated transduction of human oesophageal carcinoma cells with the interferon- λ genes produced anti-tumour effects. *Br J Cancer* 2011; **105**: 1302–12.
- 36 Hosoi T, Ozawa K. Endoplasmic reticulum stress in disease: Mechanisms and therapeutic opportunities. *Clin Sci (Lond)* 2009; **118**: 19–29.
- 37 Xu Y, Yu H, Qin H *et al.* Inhibition of autophagy enhances cisplatin cytotoxicity through endoplasmic reticulum stress in human cervical cancer cells. *Cancer Lett* 2012; **314**: 232–43.
- 38 Kim SR, Kim HJ, Kim DI *et al.* Blockade of interplay between IL-17A and endoplasmic reticulum stress attenuates LPS-induced lung injury. *Theranostics* 2015; **5**: 1343–62.
- 39 Liu WT, Huang CY, Lu IC, Gean PW. Inhibition of glioma growth by minocycline is mediated through endoplasmic reticulum stress-induced apoptosis and autophagic cell death. *Neuro Oncol* 2013; **15**: 1127–41.
- 40 Naidoo N. ER and aging-protein folding and the ER stress response. *Ageing Res Rev* 2009; **8**: 150–9.
- 41 Palam LR, Baird TD, Wek RC. Phosphorylation of eIF2 facilitates ribosomal bypass of an inhibitory upstream ORF to enhance CHOP translation. *J Biol Chem* 2011; **286**: 10939–49.
- 42 Wei Y, Sinha S, Levine B. Dual role of JNK1-mediated phosphorylation of Bcl-2 in autophagy and apoptosis regulation. *Autophagy* 2008; **4**: 949–51.
- 43 Kim I, Xu W, Reed JC. Cell death and endoplasmic reticulum stress: Disease relevance and therapeutic opportunities. *Nat Rev Drug Discov* 2008; **7**: 1013–30.
- 44 Bate-Eya LT, den Hartog IJ, van der Ploeg I *et al.* High efficacy of the BCL-2 inhibitor ABT199 (venetoclax) in BCL-2 high-expressing neuroblastoma cell lines and xenografts and rationale for combination with MCL-1 inhibition. *Oncotarget* 2016; **7**: 27946–58.